

**Quantifying Oxygen Induced Surface Enrichment of a Dilute PdAu Alloy Catalyst**

Journal:	<i>Catalysis Science & Technology</i>
Manuscript ID	CY-COM-07-2021-001337.R2
Article Type:	Communication
Date Submitted by the Author:	29-Oct-2021
Complete List of Authors:	Karatok, Mustafa; Harvard University, Department of Chemistry and Chemical Biology Madix, Robert; Harvard University, Harvard John A. Paulson School of Engineering and Applied Sciences van der Hoeven, Jessi; Harvard University, Department of Chemistry and Chemical Biology; Harvard University, Harvard John A. Paulson School of Engineering and Applied Sciences Aizenberg, Joanna; Harvard University, Department of Chemistry and Chemical Biology; Harvard University, John A. Paulson School of Engineering and Applied Sciences Reece, Christian; Harvard University, Rowland Institute at Harvard

COMMUNICATION

Quantifying Oxygen Induced Surface Enrichment of a Dilute PdAu Alloy Catalyst

Received 00th January 20xx,
Accepted 00th January 20xx

Mustafa Karatok,^a Robert J. Madix,^b Jessi E.S. van der Hoeven,^{ab} Joanna Aizenberg^{ab} and Christian Reece^{*c}

DOI: 10.1039/x0xx00000x

Dilute PdAu alloys are promising catalysts for selective oxidation and hydrogenation reactions. However, the surface composition and active site density of the minority metal, Pd, is unknown. In this study, we quantitatively determine a three-fold increase in the Pd site density on the surface of a dilute Pd_{0.08}Au_{0.92} alloy catalyst after oxygen activation by titrating the oxidized surface with quantified pulses of CO.

Dilute bimetallic catalysts are of great interest as the interplay between the two metals provides desirable catalytic properties, often surpassing those of the individual metals.¹⁻⁵ However, the dilute nature of the minority metal means that even with high resolution spectroscopic and microscopic techniques (*e.g.*, X-ray Absorption Spectroscopy, Transmission Electron Microscopy, etc.) the exact surface composition and distribution of these particles is quite difficult to resolve.^{6,7} Further, these catalysts are highly sensitive to pretreatment and reaction conditions, indicating a highly dynamic surface composition.⁸⁻¹³ A clear and concise method of probing the state of a catalyst surface is to titrate active species using precise pulses of reactants, providing both structural and kinetic insight into the nature of an activated surface.¹³⁻²² Herein, the surface Pd composition of oxygen-pretreated dilute PdAu alloy particles supported on a raspberry-colloid-templated silica (RCT-SiO₂)^{23,24} catalyst was determined using quantified pulses of CO from a Temporal Analysis of Products (TAP, see SI-1) reactor.

Dilute PdAu alloys have been shown to selectively catalyse oxidation^{6,25,26} and hydrogenation²⁷⁻³¹ reactions. In particular, dilute Pd_xAu_{1-x} (*x* < 0.1 at%) particles supported on RCT-SiO₂ were

shown to be active and selective for CO oxidation⁶, 1-hexyne hydrogenation⁸, and oxidative alcohol coupling³² reactions. In these reactions Pd activates either O₂ or H₂ to initiate the reaction cycle, and Au limits over-oxidation/hydrogenation of the reactants. In PdAu nanoparticles of uniform bulk and surface structure the Pd is atomically dispersed within the bulk of the Au nanoparticle, and only a small fraction of the Pd would be exposed to the surface. However, oxidative treatment at elevated temperatures provides a thermodynamic driving force for Pd to segregate to the surface. Increasing activity of partially deactivated Pd_xAu_{1-x}-RCT-SiO₂ catalyst after O₂ pretreatment has been demonstrated for both hydrogenation and oxidation reactions.^{8,9}

Surface science studies³³ and theoretical calculations^{8,34} provide clear indications for the Pd enrichment at the PdAu surface after O₂ treatment. However, the surface composition and surface distribution of Pd in supported particles after oxygen treatment remain unknown. Here, the oxidized Pd_{0.08}Au_{0.92}-RCT-SiO₂ was titrated using calibrated CO pulses, and then the total CO₂ formation was quantified using a mass spectrometer. The results from the TAP experiments demonstrate that a significant portion of the Pd is segregated to the surface by O₂ treatment, resulting in an enriched surface containing > 0.26 monolayer (ML) of Pd (*i.e.*, 26 atm%) on the exposed particle surface.

A Pd_{0.08}Au_{0.92}-RCT-SiO₂ catalyst was synthesized using the previously published procedure (see SI-2).¹³ For its initial oxidation, 7.4 mg of the Pd_{0.08}Au_{0.92}-RCT-SiO₂ catalyst was pretreated with dry air (Airgas, AI-D300, 20-22% of O₂ in N₂, 40-45 cm³/min) at 673 K for 30 minutes, then cooled to 553 K in the flowing air in the TAP microreactor. The sample was evacuated to 10⁻⁸ torr, and the amount of oxygen species on the surface of the catalyst was determined by titration with a sequence of quantified (see SI) pulses of a 20.84 mol% CO/Ar mixture (containing approximately 2x10¹⁴ molecules of CO in each pulse) until CO₂ production ceased. As only one *m/z* value can be scanned at a time three are required to probe the full *m/z* range of 28, 40 and 44, corresponding to CO, Ar, and CO₂,

^a Department of Chemistry and Chemical Biology, Harvard University, Cambridge, MA, USA.

^b Harvard John A. Paulson School of Engineering and Applied Sciences, Harvard University, Cambridge, MA, USA.

^c Rowland Institute at Harvard, Harvard University, Cambridge, MA, USA.

[†] Electronic Supplementary Information (ESI) available: Details of the transient pulse response experiments, synthesis of Pd_{0.08}Au_{0.92}-RCT catalyst, and calculations for number of surface atoms on particles. See DOI: 10.1039/x0xx00000x

respectively. The combination of three consecutive pulses is referred to as a pulse set. A pulse set is displayed in Figure 1, the peak maxima at $0.17 t_{dim}$ (see SI-1) for the inert response demonstrates the gas flow is within the Knudsen regime and the reactor is uniformly packed.³⁵ To quantify the amount of CO_2 produced from the oxygen titration experiments, the m/z 44 responses were integrated and scaled to the Ar marker pulse (see SI-1). The scaling coefficient (C) relating the raw mass spec signal to the number of molecules was obtained before each titration experiment (see SI-1 for calculation details).

The preoxidized $\text{Pd}_{0.08}\text{Au}_{0.92}\text{-RCT-SiO}_2$ catalyst is highly active for CO oxidation (Fig 2a). In the first pulse set, 92% of the CO molecules are converted to CO_2 (Fig 2b) clearly indicating the availability of oxygen at the surface. The CO_2 production declined with sequential CO pulses, approaching zero after approximately 200 pulse sets (600 pulses, Fig. 2a). Since the adsorption of CO to the Pd surface is completely reversible at 553 K,³⁶ and no further uptake of CO was recorded after CO_2 production had stopped, the decreasing activity is attributed to the consumption of oxygen by CO. Thermal decomposition of the oxidized surface is also not expected at 553 K during the timescale of the experiment as the decomposition temperature of both PdO ,³⁷ and chemisorbed O on Pd³⁸ are above 553 K. We do not rule out redistribution of Pd back into the bulk after reduction by CO, but as the reduced Pd has already been counted it should not affect the final result.

Using the assumption of PdO as the active surface and the production of one CO_2 per adsorbed oxygen atom, the total number of the surface Pd atoms was determined to be $1.16(\pm 0.03) \times 10^{16}$ atoms. The average particle diameter of the as-prepared catalysts is 5.6 nm, giving a total of 2.97×10^{17} surface atoms (see SI-3). In the RCT-SiO₂ catalysts, nanoparticles are embedded in the silica support, with exposed surface areas ranging from <10% up to 50% with an average of 15% of the surface exposed across the sample.³⁹ Using the average exposed surface area $\sim 4.45 \times 10^{16}$ total atoms are available at the exposed surface, of which $\sim 3.47 \times 10^{15}$ atoms of Pd are expected based on the bulk composition. Therefore, the surface Pd concentration computed from the total amount of CO_2 formed during the sequential CO pulsing experiments indicates at least a three-fold enrichment of Pd at the surface after O_2 pretreatment.

Previous DFT calculations⁸ on $\text{Pd}_{0.04}\text{Au}_{0.96}$ indicate that the most likely oxide phase to form under experimental conditions is PdO. This provides a lower limit on the amount of Pd available

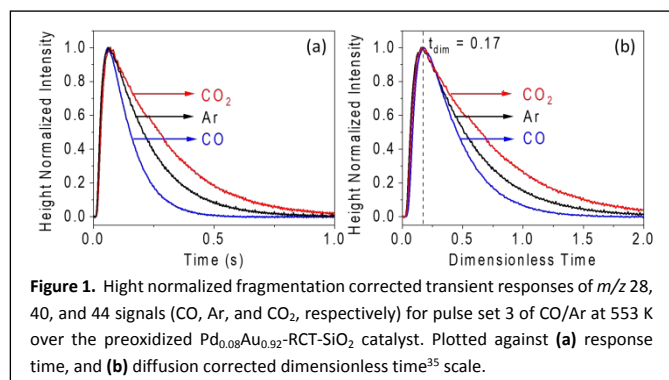


Figure 1. Height normalized fragmentation corrected transient responses of m/z 28, 40, and 44 signals (CO , Ar , and CO_2 , respectively) for pulse set 3 of CO/Ar at 553 K over the preoxidized $\text{Pd}_{0.08}\text{Au}_{0.92}\text{-RCT-SiO}_2$ catalyst. Plotted against (a) response time, and (b) diffusion corrected dimensionless time³⁵ scale.

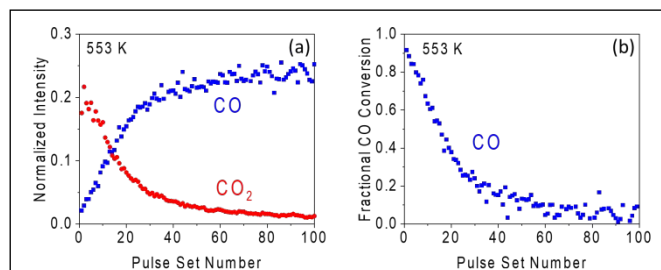


Figure 2. Sequential pulsing of a CO/Ar mixture at 553 K over the pre-oxidized $\text{Pd}_{0.08}\text{Au}_{0.92}\text{-RCT-SiO}_2$ catalyst. Each data point shows (a) the integrated area under the corresponding pulse curve normalized to the Ar response in each set, (b) the fractional CO conversion in each set.

at the surface, as higher Pd:O ratios would occur where the O is chemisorbed on 2D Pd islands. It is important to note that while Pd oxide formation with higher oxygen stoichiometry (e.g., PdO_2) has been reported, this requires extreme conditions⁴⁰ (4 GPa O_2 , >1100 K) not present during our pre-treatment. Clearly, O_2 treatment at elevated temperature draws a significant fraction of the bulk Pd atoms to the surface (assuming a Pd:O ratio of 1), resulting in a Pd coverage of ~ 0.26 ML (Table 1) vs 0.08 ML expected from the bulk Pd concentration. Analysis of a similar $\text{Pd}_{0.04}\text{Au}_{0.96}\text{-RCT-SiO}_2$ catalyst pretreated with O_2 at 673 K for 1 hour using extended X-ray absorption fine structure (EXAFS) measured a Pd-O distance longer than bulk PdO, suggesting the presence of chemisorbed oxygen on that catalyst.⁸ Note that the surface composition of that catalyst could not be resolved due to its dilute nature, although the heterogeneity of a PdAu alloy with 1:1 bulk composition was previously determined by EXAFS.⁴¹ Several two-dimensional surface oxygen phases, such as $p(2 \times 2)\text{O}$, $c(2 \times 2)\text{O}$, and $p(5 \times 5)\text{O}$ structures have been reported on Pd surfaces, which contain Pd:O ratios of 4, 2, and 1.6 respectively.³⁸ Assuming that the surface O/Pd is in the form of $p(2 \times 2)\text{O}$, this provides the upper limit of ~ 1.1 ML of Pd drawn to the surface. In that case, the exposed surface of the particles would be a Pd monolayer.

Table 1. Surface Pd coverage of nanoparticles (ML) derived using total CO_2 production from sequential CO pulses at 553 K on preoxidized $\text{Pd}_{0.08}\text{Au}_{0.92}\text{-RCT-SiO}_2$ catalyst. Five independent titrations were performed at 553 K with a reproducibility of 98%.

Run	Amount of CO_2 produced (molecules)	Exposed Surface Pd coverage	
		PdO	$p(2 \times 2)\text{O}$
1	1.22×10^{16}	0.27 ML	1.10 ML
2	1.14×10^{16}	0.26 ML	1.02 ML
3	1.14×10^{16}	0.26 ML	1.02 ML
4	1.08×10^{16}	0.24 ML	0.97 ML
5	1.23×10^{16}	0.28 ML	1.11 ML

The CO conversion in a given pulse is related to the overall rate constant for the reaction of CO with adsorbed O at that coverage, making it possible to directly measure the kinetics of CO oxidation as a function of the changing surface coverage. The Thin-Zone-TAP-Reactor configuration employed here acts as a diffusionally-mixed reactor (CSTR).⁴² Consequently, an apparent rate constant, k_{app} , for the CO oxidation titration reaction can be calculated from the fractional CO conversion (X)

and assuming pseudo-first order kinetics with respect to CO concentration:

$$k_{app} = \frac{X}{1 - X\tau_{cat}} \quad (1)$$

$$\tau_{cat} = \varepsilon \left(\frac{L_{cat}L_{in2}}{D} \right) \quad (2)$$

$$D = \frac{\varepsilon d_i (\delta RT)}{3\tau (\pi M)}^{1/2} \quad (3)$$

with τ_{cat} being the mean residence time of CO in the catalyst zone, L_{cat} and L_{in2} being the lengths of the catalyst zone and the second inert zone respectively, and ε being the void fraction of the packed bed. The diffusivity D is dependent on the diameter of the interstitial voids d_i , the tortuosity of the bed τ , the temperature T and the molecular weight of the gas M , and R is the universal gas constant. As the same catalyst bed is used for all experiments the characteristics of the catalyst bed remains the same for all pulses, and changes in k_{app} are directly related to the inherent rate constant for the titration reaction. Therefore, the apparent rate constant can be derived by using the following relation:

$$k'_{app} = \frac{X}{1 - X} \sqrt{T} \approx k_{app} \quad (4)$$

The apparent rate constant k'_{app} calculated using eqn (4) decreases linearly as the adsorbed O is consumed and CO₂ is produced (Fig. 3). The two linearly changing regimes with substantially different slopes indicate two different rate constants for the reaction, which can correlate to two different states of the surface as O is removed.¹⁵

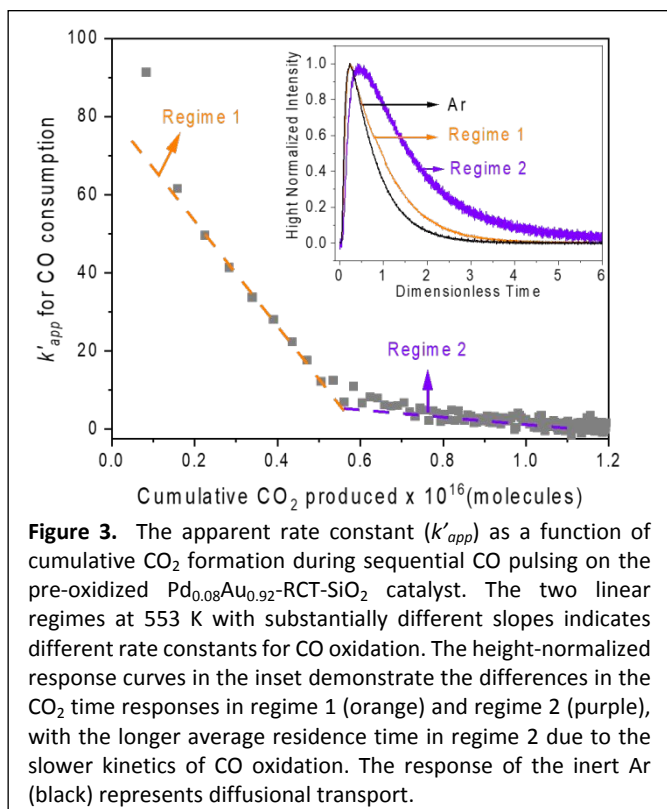


Figure 3. The apparent rate constant (k'_{app}) as a function of cumulative CO₂ formation during sequential CO pulsing on the pre-oxidized Pd_{0.08}Au_{0.92}-RCT-SiO₂ catalyst. The two linear regimes at 553 K with substantially different slopes indicates different rate constants for CO oxidation. The height-normalized response curves in the inset demonstrate the differences in the CO₂ time responses in regime 1 (orange) and regime 2 (purple), with the longer average residence time in regime 2 due to the slower kinetics of CO oxidation. The response of the inert Ar (black) represents diffusional transport.

Although accurate measurements of the diffusion coefficients were not recorded experimentally, it is possible to generate an approximation of the apparent rate constant using estimates of the diffusivity, reactor voidage, and tortuosity using eqns (5)-(8). The diameter of the interstitial voids can be related to the catalyst particle diameter (d_p) using:

$$d_i = \frac{2\varepsilon}{3(1-\varepsilon)} d_p \quad (5)$$

with an average catalyst particle diameter of 200 μm and a void fraction of 0.5, the diameter of the interstitial voids can be estimated to be 8×10^{-5} cm. Assuming a tortuosity of 2 the Knudsen diffusion coefficient can be estimated to be $43.11 \text{ cm}^2\text{s}^{-1}$ for CO at 553 K using eqn (3). Then, the residence time in the catalyst zone can then be calculated as 0.0281s (eqn. (2)). Finally, the apparent rate constant is approximated using eqn (1). Using the approximated apparent rate constant, the intrinsic rate constant for CO oxidation can then be calculated for the two regimes assuming a pseudo first-order reaction and using the following relationship.³⁵

$$k_{app} = \frac{\sigma a_v (1 - \varepsilon)}{\varepsilon} k_a \quad (6)$$

where a_v is the specific surface area (cm^2/cm^3), σ is the surface site density (mol/cm^2), and k_a is the intrinsic rate constant for adsorption/reaction of CO ($\text{cm}^3\text{mol}^{-1}\text{s}^{-1}$). A plot of apparent rate constant vs the number of adsorbed O sites provides a slope of

$$\frac{\Delta k_{app}}{\Delta \theta_{O^*}} = \frac{(1 - \varepsilon)}{\varepsilon V} k_a \quad (7)$$

where V is the volume of the catalyst zone, and θ_{O^*} is the number of adsorbed O sites. For regime 1 (Figure 3) the intrinsic rate constant for adsorption/reaction is estimated to be $10^{-16} \text{ cm}^3\text{mol}^{-1}\text{s}^{-1}$ and for regime 2 (Figure 3) the intrinsic rate constant for adsorption/reaction is estimated to be $10^{-17} \text{ cm}^3\text{mol}^{-1}\text{s}^{-1}$. The adsorption/reaction rate constant for a Knudsen TAP pulse is defined as⁴³

$$k_a = \frac{P_{reaction}}{\sigma} \sqrt{\frac{RT}{2\pi M}} \quad (8)$$

Where $P_{reaction}$ is the reaction probability of CO with an O site. Assuming a site density between 1×10^{18} to 1×10^{19} sites/ m^2 the reaction probability of CO with O adsorbed on the Pd_{0.08}Au_{0.92}-RCT-SiO₂ catalyst can be estimated to be $\sim 10^{-5}$ and $\sim 10^{-6}$ for regimes 1 and 2, respectively.

Two distinct reaction pathways for CO oxidation have been reported on a PdO(101) surface.⁴⁴ The first of which is the facile oxidation of CO adsorbed on coordinatively unsaturated Pd atoms with neighbouring O. As the surface continues to be reduced, the CO migrates to the created oxygen vacancy sites, binding more strongly, and the reaction becomes less facile. Two pathways are also observed in the transient response of CO₂ (Figure 3 – inset). In Regime 1, the exit flux of the CO₂ response is initially limited by the diffusional transport through

the bed, indicating an instantaneous reaction of CO with adsorbed O and desorption of CO₂; after the peak there is a tailing of the CO₂ response indicating a slower reaction process limiting the exit of CO₂ from the reactor.¹⁵ In Regime 2, the CO₂ response is much broader than the diffusional transport response indicating a slower reaction of CO with adsorbed O. The instantaneous release of CO₂ coupled with the tailing CO₂ response at high coverages in Regime 1 indicates that both sites are present and active simultaneously, with the more active site decaying more rapidly leaving only the less active site at low O coverage. The less active oxygen here could either be the one in Pd oxide structure reacting with CO on the oxygen vacancy sites, or an adsorbed O on Pd that is generated by the decomposition of the Pd oxide phase upon fast reduction.

Conclusions

In this work, we have determined the oxygen coverage over an oxidized Pd_{0.08}Au_{0.92}-RCT-SiO₂ catalyst by titrating the oxygen with quantified CO pulses. Using known stoichiometries of oxidized Pd surfaces, we calculate that the surface Pd concentration after oxygen pre-treatment is enhanced between 3.3 and 13.2 times relative to the bulk composition. Kinetic analysis of the CO conversion as a function of oxygen coverage suggests that there are two sites for CO oxidation on the oxidized Pd_{0.08}Au_{0.92}-RCT-SiO₂. The findings emphasize the highly dynamic nature of these bimetallic systems and demonstrate how the surface state can be tuned via pretreatment procedures. Further, the TAP pulse titration technique provides a direct method of quantifying the number of active species on a surface while simultaneously providing kinetic insight, that is readily transferrable to other catalytic systems.

Conflicts of interest

There are no conflicts to declare.

Acknowledgements

This work was supported as part of the Integrated Mesoscale Architectures for Sustainable Catalysis (IMASC), an Energy Frontier Research Center funded by the U. S. Department of Energy, Office of Science, Basic Energy Sciences under Award No. DE-SC0012573. CR gratefully acknowledges the Rowland Fellowship through the Rowland Institute at Harvard. The authors gratefully acknowledge Dr. Michael Aizenberg for his careful reading of the manuscript.

Author Contributions

MK conducted the TAP experiments and analysed the data with guidance from CR. JvdH synthesized and characterized the catalysts, guided by JA. RJM and CR guided the research. MK

wrote the manuscript together with CR with contributions from all of the authors. All authors participated in discussions.

Notes and references

- 1 J. H. Sinfelt, *Acc. Chem. Res.*, 1976, 10, 15–20.
- 2 M. Sankar, N. Dimitratos, P. J. Miedziak, P. P. Wells, C. J. Kiely and G. J. Hutchings, *Chem. Soc. Rev.*, 2012, 41, 8099–8139.
- 3 D. M. Alonso, S. G. Wettstein and J. A. Dumesic, *Chem. Soc. Rev.*, 2012, 41, 8075–8098.
- 4 G. Giannakakis, M. Flytzani-Stephanopoulos and E. C. H. Sykes, *Acc. Chem. Res.*, 2019, 52, 237–247.
- 5 R. T. Hannagan, G. Giannakakis, M. Flytzani-Stephanopoulos and E. C. H. Sykes, *Chem. Rev.*, 2020, 120, 12044–12088.
- 6 M. Luneau, T. Shirman, A. Filie, J. Timoshenko, W. Chen, A. Trimpalis, M. Flytzani-Stephanopoulos, E. Kaxiras, A. I. Frenkel, J. Aizenberg, C. M. Friend and R. J. Madix, *Chem. Mater.*, 2019, 31, 5759–5768.
- 7 N. Marcella, Y. Liu, J. Timoshenko, E. Guan, M. Luneau, T. Shirman, A. M. Plonka, J. E. S. Van Der Hoeven, J. Aizenberg, C. M. Friend and A. I. Frenkel, *Phys. Chem. Chem. Phys.*, 2020, 22, 18902–18910.
- 8 M. Luneau, E. Guan, W. Chen, A. C. Foucher, N. Marcella, T. Shirman, D. M. A. Verbart, J. Aizenberg, M. Aizenberg, E. A. Stach, R. J. Madix, A. I. Frenkel and C. M. Friend, *Commun. Chem.*, 2020, 3, 1–9.
- 9 A. Filie, T. Shirman, M. Aizenberg, J. Aizenberg, C. M. Friend and R. J. Madix, *Catal. Sci. Technol.*, 2021, 11, 4072–4082.
- 10 F. Tao, M. E. Grass, Y. Zhang, D. R. Butcher, J. R. Renzas, Z. Liu, J. Y. Chung, B. S. Mun, M. Salmeron and G. A. Somorjai, *Science*, 2008, 322, 932–935.
- 11 F. Gao, Y. Wang and D. W. Goodman, *J. Am. Chem. Soc.*, 2009, 131, 5734–5735.
- 12 S. Han and C. B. Mullins, *ACS Catal.*, 2018, 8, 3641–3649.
- 13 J. E. S. van der Hoeven, H. T. Ngan, A. Taylor, N. M. Eagan, J. Aizenberg, P. Sautet, R. J. Madix and C. M. Friend, *ACS Catal.*, 2021, 11, 6971–6981.
- 14 L. C. Wang, C. M. Friend, R. Fushimi and R. J. Madix, *Faraday Discuss.*, 2016, 188, 57–67.
- 15 S. O. Shekhtman, A. Goguet, R. Burch, C. Hardacre and N. Maguire, *J. Catal.*, 2008, 253, 303–311.
- 16 C. Reece, E. A. Redekop, S. Karakalos, C. M. Friend and R. J. Madix, *Nat. Catal.*, 2018, 1, 852–859.
- 17 D. Widmann, Y. Liu, F. Schüth and R. J. Behm, *J. Catal.*, 2010, 276, 292–305.
- 18 Y. Wang, F. Kapteijn and M. Makkee, *Appl. Catal. B Environ.*, 2018, 231, 200–212.
- 19 K. Morgan, B. Inceesungvorn, A. Goguet, C. Hardacre, F. C. Meunier and S. O. Shekhtman, *Catal. Sci. Technol.*, 2012, 2, 2128–2133.
- 20 M. Olea, M. Tada, Y. Iwasawa, V. Balcaen, I. Sack, G. B. Marin, D. Poelman and H. Poelman, *J. Chem. Eng. Japan*, 2009, 42, 219–225.
- 21 E. A. Redekop, G. S. Yablonsky, D. Constales, P. A. Ramachandran, C. Pherigo and J. T. Gleaves, *Chem. Eng. Sci.*, 2011, 66, 6441–6452.
- 22 H. Nishiguchi, H. Yamada, M. Ogura, T. Ishihara and Y. Takita, *Res. Chem. Intermed.*, 2003, 29, 755–760.
- 23 E. Shirman, T. Shirman, A. V. Shneidman, A. Grinthal, K. R. Phillips, H. Whelan, E. Bulger, M. Abramovitch, J. Patil, R. Nevarez and J. Aizenberg, *Adv. Funct. Mater.*, 2018, 28, 1–20.
- 24 Aizenberg et al., *US Pat.*, 10 265 694, 2019.
- 25 T. Ward, L. Delannoy, R. Hahn, S. Kendell, C. J. Pursell, C. Louis and B. D. Chandler, *ACS Catal.*, 2013, 3, 2644–2653.
- 26 C. J. Wrasman, A. Boubnov, A. R. Riscoe, A. S. Hoffman, S. R. Bare and M. Cargnello, *J. Am. Chem. Soc.*, 2018, 140, 12930–12939.

- 27 A. Hugon, L. Delannoy, J. M. Krafft and C. Louis, *J. Phys. Chem. C*, 2010, 114, 10823–10835.
- 28 J. Liu, J. Shan, F. R. Lucci, S. Cao, E. C. H. Sykes and M. Flytzani-Stephanopoulos, *Catal. Sci. Technol.*, 2017, 7, 4276–4284.
- 29 M. Luneau, T. Shirman, A. C. Foucher, K. Duanmu, D. M. A. Verbart, P. Sautet, E. A. Stach, J. Aizenberg, R. J. Madix and C. M. Friend, *ACS Catal.*, 2020, 10, 441–450.
- 30 P. Concepción, S. García, J. C. Hernández-Garrido, J. J. Calvino and A. Corma, *Catal. Today*, 2016, 259, 213–221.
- 31 T. Ricciardulli, S. Gorthy, J. S. Adams, C. Thompson, A. M. Karim, M. Neurock and D. W. Flaherty, *J. Am. Chem. Soc.*, 2021, 143, 5445–5464.
- 32 A. Filie, T. Shirman, A. C. Foucher, E. A. Stach, M. Aizenberg, J. Aizenberg, C. M. Friend and R. J. Madix, *J. Catal.*, DOI:10.1016/j.jcat.2021.06.003.
- 33 M. C. Saint-Lager, M. A. Languille, F. J. Cadete Santos Aires, A. Bailly, S. Garaudee, E. Ehret and O. Robach, *J. Phys. Chem. C*, 2018, 122, 22588–22596.
- 34 B. Zhu, G. Thrimurthulu, L. Delannoy, C. Louis, C. Mottet, J. Creuze, B. Legrand and H. Guesmi, *J. Catal.*, 2013, 308, 272–281.
- 35 J. T. Gleaves, G. S. Yablonskii, P. Phanawadee and Y. Schuurman, *Appl. Catal. A Gen.*, 1997, 160, 55–88.
- 36 M. Morkel, G. Rupprechter and H. J. Freund, *J. Chem. Phys.*, 2003, 119, 10853–10866.
- 37 J. A. Hinojosa and J. F. Weaver, *Surf. Sci.*, 2011, 605, 1797–1806.
- 38 S. L. Chang and P. A. Thiel, *J. Chem. Phys.*, 1988, 88, 2071–2082.
- 39 J. E. S. van der Hoeven, S. Kraemer, S. Dussi, T. Shirman, K.-C. K. Park, C. H. Rycroft, D. C. Bell, C. M. Friend and J. Aizenberg, *Adv. Funct. Mater.*, 2021, DOI: 10.1002/adfm.202106876
- 40 S. F. Matar, G. Demazeau, M. H. Möller and R. Pöttgen, *Chem. Phys. Lett.*, 2011, 508, 215–218.
- 41 S. N. Reifsnnyder and H. H. Lamb, *J. Phys. Chem. B*, 1999, 103, 321–329.
- 42 S. O. Shekhtman, G. S. Yablonsky, S. Chen and J. T. Gleaves, *Chem. Eng. Sci.*, 1999, 54, 4371–4378.
- 43 Y. Schuurman, *Catal. Today*, 2007, 121, 187–196.
- 44 F. Zhang, L. Pan, T. Li, J. T. Diulus, A. Asthagiri and J. F. Weaver, *J. Phys. Chem. C*, 2014, 118, 28647–28661.